Int J Clin Exp Med 2016;9(7):12896-12903
www.ijcem.com /ISSN:1940-5901/IJCEM0019778

Original Article

Correlations between computed tomography perfusion enhancement parameters and lymph node metastasis in non-small cell lung cancer

Shengli Zhou, Yan Gu, Gang Yuan, Zongsheng Wang, Lianqing Huang

Department of Radiology, The First People's Hospital of Lianyungang, Lianyungang 222000, Jiangsu Province, China

Received November 15, 2015; Accepted June 5, 2016; Epub July 15, 2016; Published July 30, 2016

Abstract: This study aims to study the values of computed tomography (CT) perfusion enhancement parameters (CT-PEPs) in predicting lymph node metastasis (LNM) of lung cancer. A total of 80 patients with non-small cell lung cancer (NSCLC) underwent CT perfusion scanning. CT-PEPs were calculated according to the time-density curve (TDC) in the first-pass phase, and microvessel density (MVD) was determined to analyze the diagnostic efficacies of MVD and CT-PEPs in evaluating LNM of lung cancer. MVD in the LNM group was higher than that in the non-LNM group [(59.66±6.82) vs. (49.81±7.76)/0.74 mm^2, $P < 0.05$), and the blood volume (BV) of the tumor mass in the LNM group was higher than that in the non-LNM group [(9.00±3.12) vs. (5.97±2.76) ml·100 g^{-1}, $t = -4.529$, $P < 0.05$)]. MVD ≥ 54/0.74 mm^2 or BV ≥ 7 ml·100 g^{-1} had high sensitivity and specificity (83% and 83%; 78% and 83%, respectively) for strongly suggesting the possibility of LNM of lung cancer. Among CT-PEPs, BV could be an important parameter for the preoperative judgment of LNM of lung cancer.

Keywords: Lung cancer, pathology, lymph node metastasis, perfusion imaging, tomography, X-ray computer

Introduction

Non-small cell lung cancer (NSCLC), which accounts for 80%-85% of lung cancer, is a malignant tumor with high incidence and high mortality [1]. Despite a multitude of treatment approaches over the years, including surgery, chemotherapy, and radiation, the 5-year survival rate of NSCLC patients has increased only by 15% [2], with the majority of patients dying within a year of diagnosis [3]. As long as metastasis occurs, the benefit rate to patients is very low despite the treatment type. The only way to improve long-term disease-free survival and to achieve an almost 100% 5-year survival rate is to resect non-metastatic tumors in the early stage [4, 5]. Therefore, the existence of metastasis is a watershed shift in NSCLC treatment. In various metastatic pathways, the lymph nodes are one of the most common sites of metastasis. Studies have shown that even in patients with stage III NSCLC, the 5-year survival rate is 35% as long as lymph node metastasis (LNM) has not occurred [6, 7]. LNM is therefore an important factor affecting patients' prognosis. Studies in this field most commonly use the criterion of "shortest diameter of lymph node > 10 mm" in computed tomography (CT) and magnetic resonance imaging (MRI) to indicate metastasis, but the judgment efficacy of this method is often unsatisfactory. Because certain studies have shown that lymph node size is not related to metastasis, preoperative examination of lymph node morphology alone would have a certain degree of error in determining whether metastasis exists [8]. With the recent introduction of new lung cancer staging methods that abandon simple pathological staging methods by combining CT findings with pathologic manifestations for staging prediction [9-12], CT has attained greater importance. In recent years, the use of angiogenetic conditions in primary tumors to evaluate the biological behavior of NSCLC has become a new hotspot in the medical imaging field. This approach can quantitatively assess tumor stage [13] and evaluate the treatment efficacy before and after chemotherapy [14, 15].

However, so far, few studies have investigated the use of CT perfusion (CTP) in predicting potential LNM. CTP techniques can reflect angiogenesis to a certain extent, and thus have been widely used to study tumor responses to treatment and to evaluate tumoral microvessels, as angiogenesis plays a key role in tumor metastasis [16]. Studies have shown that microvessel density (MVD) in lung cancer is related with LNM and prognosis [17, 18], indicating that MVD could be effective for assessing the malignant behavior and LNM potential of lung cancer. However, there are still some limitations in applying MVD detection assays in clinical practice; therefore, the use of radiographic parameters to assess the LNM potential of lung cancer would certainly have clinical significance. This study investigated the correlations between CT perfusion enhancement parameters (CT-PEPs) and LNM of lung cancer, and further, the value of CT-PEPs in predicting LNM of lung cancer, to provide a reference for better diagnosis and treatment of NSCLC.

Materials and methods

Clinical data

This study included patients admitted to our hospital from May 2011 through May 2014 for CT perfusion examination due to solitary pulmonary space-occupying lesions. None of the patients had undergone any anti-tumor therapy. The study was approved by the hospital ethics committee, and written informed consent was obtained from all participants before examination. A total of 108 patients underwent CT perfusion scanning, including 97 patients with NSCLC. Of these, 82 patients underwent radical resection of lung cancer within 1 week of CTP, 10 refused surgery and chose neoadjuvant chemotherapy, 4 did not undergo surgery within 1 week of CTP, and CT perfusion scans failed in 5 due to poor respiratory cooperation. Finally, 80 patients who underwent radical resection of lung cancer within 1 week of CTP and had complete surgical records and pathological reports (including LNM that were removed) were enrolled into the study. The patients were divided into two groups on the basis of pathological results: patients with LNM (the LNM group) and without LNM (the non-LNM group). This study was conducted in accordance with the declaration of Helsinki. This study was conducted with approval from the Ethics Committee of the First People's Hospital of Lianyungang. Written informed consent was obtained from all participants.

Inclusion and exclusion criteria

Inclusion criteria were the following: solitary spacing-occupying lesion with a maximum diameter ≥ 1 cm in lungs, could cooperate with the examination after breathing training, could withstand a high injection rate of contrast agent, absence of allergy, and absence of other parenchymal organ metastasis on imaging examination.

Exclusion criteria were the following: obvious benign coarse calcification or fat-containing space-occupying lesion, pure ground-glass-like dense nodes, and inability to cooperate with breathing during the examination (which would prevent calculation of the perfusion value).

Preoperative CTP examination and image analysis

Breathing training was performed in all patients before CT scanning. Patients were asked to breathe calmly and refrain from swallowing. A Light Speed Ultra 16-slice CT (GE Healthcare, the USA) was first used to perform conventional CT for lesions with a layer thickness of 5 mm; next, we chose the four layers adjacent to the lesion center that had the same diameter as the target layer, and performed CT perfusion scanning with "toggling-table" technology. A total dose of 50 mL of the non-ionic contrast agent ioversol (300 mg I/mL; Jiangsu Hengrui Co., Lianyungang, China) was injected through the cubital vein with a flow rate of 4 mL/sec. Scanning parameters were as follows: 120 kV, 80 mA, 1 sec/slice, 5 mm/4i, scanning delay 5.0 sec, data acquisition time 60 sec, average radiation dose 3.47±0.69 mSv. A total of 240 perfusion images were obtained.

After scanning, the data were imported into an ADW 4.5 workstation (GE Healthcare) for mapping, analysis, and calculations using the Perfusion 4D software package (Version 4.3, GE Healthcare). The descending aorta was used as the inflow artery when it was in the same layer as the lesion; if the lesion was located on the layer above the aortic arch, the brachiocephalic or left common carotid artery was

Table 1. Clinical information of the 80 NSCLC patients

Item	All patients	Non-LNM group	LNM group	P
Age	57.6 (30~79)	53.8 (30~71)	60.2 (37~79)	0.512
Gender				0.841
Male	47	21	26	
Female	33	14	19	
Pathological type				0.308
Squamous cell carcinoma	36	18	18	
Adenocarcinoma	44	17	27	
Tumor history in first-degree relatives				0.055
Yes	32	13	19	
No	48	30	18	
Lung cancer history in first-degree relatives				0.465
Yes	18	5	13	
No	14	6	8	
Smoking history*				0.386
Yes	51	23	28	
No	29	16	13	

*Smoking history referred to smoked ≥ 1 cigarette per day and continuously smoked for more than six months.

selected as the inflow artery for the detection of the corresponding blood flow (BF), blood volume (BV), mean transit time (MTT), and permeability surface (PS). Three to five regions of interest (ROIs) of the lesions were then selected by one high-level attending physician to obtain the corresponding perfusion parameters and their averages. ROIs were selected as large as possible using the hand-drawing method, about 1 mm away from the lesion edge and avoiding regions with necrosis (CT value < 10 Hu) and artifacts (because lesions would appear as strips in motion artifacts).

Postoperative MVD counting

All patients underwent lobectomy and dissection of the corresponding lymph nodes in the lung fissure, lung hilum, and mediastinum, performed by two experienced physicians from the department of thoracic surgery of our hospital. During surgery, the resected specimens were immediately labeled and put into sample bags for pathological evaluation. All pathological specimens were sampled by one high-level attending physician from the department of pathology, with the samples made as consistent as possible with the ROIs from CT imaging (e.g., excluding necrotic and calcified sections). Samples were then fixed in formalin and embedded in paraffin for future evaluation. Vessels were detected with a monoclonal antibody against the vascular endothelial cell surface antigen CD34 using the MaxVision quick immunohistochemical staining method (MaxVision Biosciences, Kenmore, WA, USA) according to the manufacturer's instructions. MVD was then calculated as follows: the whole stained section was viewed under low magnification (40×), the visual field with the most stained vascular endothelial cells (vascular hotspot) was selected, and the number of microvessels in 3 visual fields under high magnification (400×) was counted; the average value was then used as the MVD.

MVD was counted using the Weidner method, in which the absence of red blood cells and lumen is prerequisite to microvessel determination. Several brown-stained endothelial cells or endothelial cell clusters were counted as a microvessel, while vessels with a lumen diameter larger than the width of 8 red blood cells and a thick muscular layer, as well as those in sclerotic regions, were not counted. The results were judged by two physicians using the double-blind method, and the average was used as the final count.

Statistical analysis

SPSS statistical software (Version 16.0, IBM Corporation, Armonk, NY, USA) was used for the analysis. Comparison of CT-PEPs and NSCLC MVD between the LNM group and the non-LNM group was performed using the group *t* test or *t* test, with $P < 0.05$ considered as statistically significant. Linear correlation analysis was used to evaluate the correlations between multi-slice computed tomography (MSCT)-PEPs and NSCLC MVD. The receiving operator characteristic (ROC) curve was used to analyze the

Table 2. Correlations between CTP-PEPs and MVD in NSCLC

CT-PEPs	$\bar{x} \pm s$	Range	MVD	
			r	P
BF [ml/(100 g·min)]	78.62±47.70	6.87~209.74	0.289	0.009
BV (ml/100 g)	7.68±3.31	2.66~19.18	0.894	0.001
MTT (s)	11.74±7.03	1.99~30.75	0.135	0.233
PS [ml/(100 g·min)]	14.62±10.50	2.17~51.54	0.482	0.000

difference in efficacy of the histological method compared with CT-PEPs in evaluating NSCLC-LNM, and select the best diagnostic cutoff values.

Results

Pathological results

The 80 patients (47 males, 33 females aged 30-79 years; mean age 57.6 years) were divided into the LNM group (45 cases) and the non-LNM group (35 cases) according to their pathological results.

The LNM group included 18 cases of squamous cell carcinoma and 27 cases of adenocarcinoma. The maximum diameters of lung lesions in this group ranged from 1.4 to 4.5 cm (mean 2.38±0.81 cm). Fourteen of these patients were in stage IIA, 29 were in stage IIB, and 2 patients were in stage IIIA.

The non-LNM group included 18 cases of squamous cell carcinoma and 17 cases of adenocarcinoma. The maximum diameters of lung lesions in this group ranged from 1.1 to 4.1 cm (mean 2.61±0.76 cm). Six of these patients were in stage IIA, 9 were in stage IIB, and 20 were in stage IIIA (**Table 1**).

Results of CT enhancement scanning

Compared with using the postoperative pathological results and "shortest diameter of lymph node > 10 mm" as the diagnostic criteria of LNM, 26 LNM cases were correctly diagnosed and 22 cases were correctly identified as having no LNM. Eighteen cases were misdiagnosed as having LNM but had no swelled lymph node in the mediastinum, and 14 cases were misdiagnosed as having no LNM but were confirmed as reactive hyperplasia by postoperative pathology, with lymph node diameter > 10 mm. The diagnostic sensitivity, specificity, coincidence rate, positive predictive value, and negative predictive value were 59%, 61%, 60%, 65%, and 55%, respectively.

MVD staining results in the 80 NSCLC cases

Immunohistochemical staining of samples from NSCLC patients in this study showed that the tumor interstitial substances were rich in tumoral microvessels; endothelial cells with positive CD34 staining were brown and clearly displayed, appearing as dots, lines, rings with branches or lumens, and long tubes, as well as stained endothelial cell clusters. The average MVD of all patients with NSCLC was 55.35±8.72 vessels/0.74 mm^2. Average MVDs in the LNM group and the non-LNM group were 59.66±6.82 and 49.82±7.76 vessels/0.74 mm^2, respectively. MVD in the LNM group was higher than that in the non-LNM group, and the difference was statistically significant ($t = -6.027$, $P < 0.001$).

Correlations between CTP-PEPs and MVD in NSCLC

Pearson correlation analysis of CTP-PEPs and MVD in the 80 patients with NSCLC revealed that all data were normally distributed; moreover, BV was positively correlated with MVD, while MTT, BF, and PS had no correlation with MVD (**Table 2**).

Correlations among CT-PEPs, lesion size, and LNM in NSCLC

Among CT-PEPs, BC of the LNM group was higher than that of the non-LNM group (**Figures 1**, **2**) and the difference was statistically significant ($P < 0.01$), while BF, MTT, PS, and primary tumor sizes between the LNM group and the non-LNM group were not significantly different ($P > 0.05$, **Table 3**).

Diagnostic efficacies of CT-PEPs and MVD in determining NSCLC-LNM

This study selected MVD and BV as the indexes to judge NSCLC-LNM. The AUCs of their ROC curves were 0.895 and 0.873, respectively (**Figure 3**), and the difference was not statistically significant ($\chi^2 = 0.402$, $P > 0.05$). The best diagnostic thresholds of MVD and BV for NSCLC-LNM determination were then selected by ROC, and it was found that when MVD ≥ 54

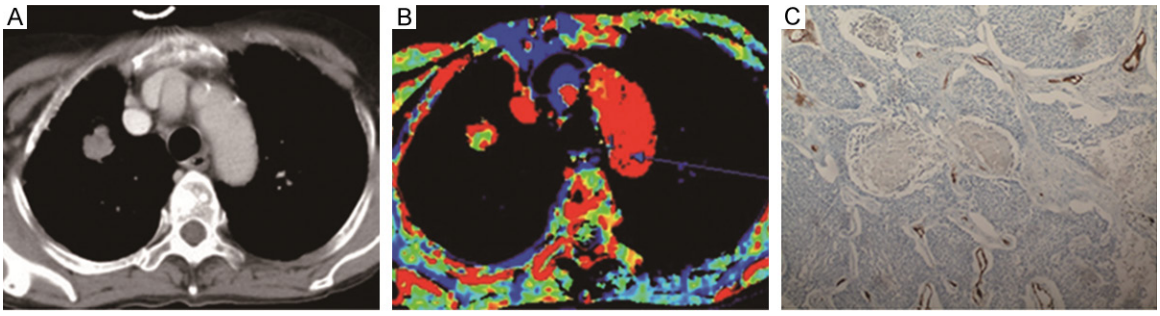

Figure 1. Adenocarcinoma in patient with no lymph node metastasis. A. A mass lesion originating from the right upper lung; B. Blood volume map (BV); C. MVD were detected by CD34 (SP×400).

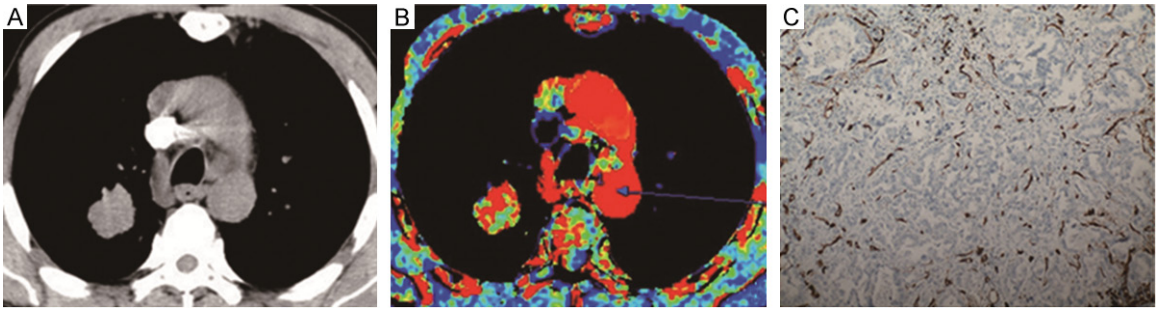

Figure 2. Lymph nodes in patient with adenocarcinoma. There is one node laterally to the main bronchus, on the right side (group 4R). High values of blood volume was suggestive for metastatic character. This node on histological examination was proven to be metastatic. A. A mass lesion originating from the right lower lung, with lymphatic metastasis on group 4R; B. Blood volume map (BV); C. MVD were detected by CD34 (SP×100).

vessels/0.74 mm^2 was set as the diagnostic threshold for LNM determination, the sensitivity was 83%, the specificity was 83%, the diagnostic coincidence rate was 85%, and the positive and negative predictive values were 87% and 83%, respectively. When BV ≥ 7 mL·100 g^{-1} was set as the diagnostic threshold for LNM determination, the sensitivity was 78%, the specificity was 83%, the diagnostic coincidence rate was 80%, and the positive and negative predictive values were 85% and 74%, respectively.

Discussion

Tateishi et al [19] studied the correlations of angiogenesis in lung tumor and dynamic contrast-enhanced CT and found that the peak height (PH) of lung adenocarcinoma was positively correlated with MVD. Trojanowski et al [20] studied lymph nodes in laryngeal cancer and also reported that among CT-PEPs, BF, BV, and PS could effectively predict LNM. When CT-PEPs were applied to predict NSCLC-LNM in the present study, BC was found to be positively correlated with MVD in NSCLC, and the BV value of the LNM group was significantly higher than that of the non-LNM group ($P < 0.01$). When ROC curve analysis was performed for MVD and BV, the diagnostic efficacies of these two factors were found to be equivalent, with no statistically significant difference. When MVD ≥ 54 vessels/0.74 mm^2 was set as the diagnostic threshold for LNM determination, the sensitivity and specificity were 83% and 83%, respectively; when BV ≥ 7 mL·100 g^{-1} was set as the diagnostic threshold, the sensitivity and specificity were 78% and 83%, respectively. These results indicate that BV and MVD could both be effective indexes for the prediction of LNM, and that higher BV values suggest a higher possibility of LNM.

Although many studies of NSCL-LNM prediction have been performed by researchers in China and other countries, CT or MRI is still the most commonly used method, with “shortest diameter of lymph node > 10 mm” set as the standard of LNM [21, 22]. However, some studies

Table 3. Correlations between each observation index and LNM

Observation index	LNM group	Non-LNM group	P
BF [ml/(100 g·min)]	84.15±47.52	71.51±47.67	0.242
BV (ml/100 g)	9.00±3.12	5.97±2.76	<0.001
MTT (s)	12.39±6.70	10.91±7.46	0.354
PS [ml/(100 g·min)]	15.56±10.20	12.56±9.45	0.182
Mass diameter (cm)	2.38±0.81	2.61±0.76	0.194
MVD (numbers/0.74 mm^2)	59.66±6.82	49.82±7.76	<0.001

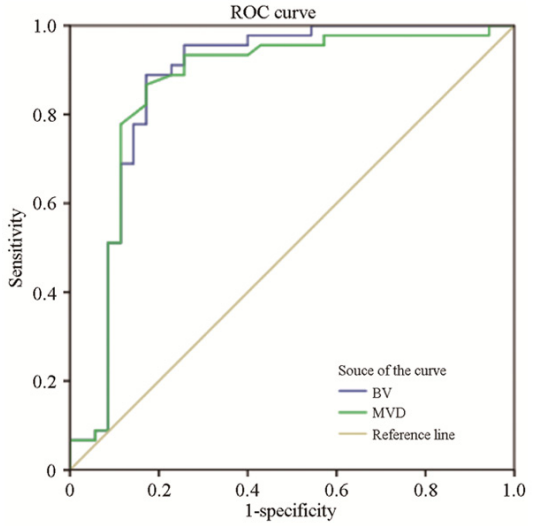

Figure 3. ROC curves.

have found that lymph node size is not related with LNM [23, 24].

In the present study, if the above standard was used, the diagnostic coincidence rate was 60%, with sensitivity of 59%, specificity of 61%, positive predictive value of 65%, and negative predictive value of 55%. The location of lymph nodes was the main reason for false-negative results; for example, the lymph nodes in the left mediastinum (2 L, 4 L, IOL, 5) and 7th station could be easily misdiagnosed due to lack of fat or the partial volume effects of peripheral vessels. On the other hand, larger lymph nodes might result from reactive hyperplasia, which could cause false-positive results. Therefore, relying simply on lymph node size was insufficient to provide reliable pretreatment staging.

Pirronti et al [25] proposed that regardless of lymph node size, the appearance of phenomena such as central low-density regions, high-density strips or nodes, thin or thick wheel wheel-rim appearance, or diffuse enhancement in enhanced spiral CT might indicate metastasis, and that lymph nodes with uniform density less than 10 mm in diameter should be considered normal, while those greater than 10 mm should be considered reactive hyperplasia. However, these morphological indexes have their own inherent flaws, which do not take into account the internal functional characteristics of tumors; therefore, their reliabilities and sensitivities are still relatively low [26]. Other studies have focused on the pathologies of postoperative or biopsy specimens [27-31], but these experimental processes were complex and difficult for wide clinical application; furthermore, the invasiveness of these methods could have negative physical and psychological effects for patients.

MSCT perfusion imaging can noninvasively and conveniently reflect intratumoral angiogenesis and function; therefore, it could become an important component of clinical and biological staging and grading of tumors, thus providing more comprehensive and accurate information for tumor treatment and prognostic evaluation.

This study also had some shortcomings. First, CT perfusion imaging is an examination method that requires higher radiation exposure; although the current was reduced in this study, the radiation dose was still higher than that of conventional CT scanning. Second, this study did not include large-cell lung cancer, which is relatively rare. Third, the target population comprised patients in whom early lung cancer was detected during surgery; therefore, the efficacy of this method in early lung cancer screening could not be evaluated.

In conclusion, our study showed that higher BV is associated with greater possibility of LNM, and that BV could become a good index for predicting angiogenesis and LNM of lung cancer. This parameter could play an increasingly important role in correct preoperative assessment of LNM status in lung cancer, thus reducing unnecessary lymph node scavenging.

Acknowledgements

This study was supported by Jiangsu Natural Science Foundation (No. SBK201122841).

Disclosure of conflict of interest

None.

Address correspondence to: Dr. Yan Gu, Department of Radiology, The First People's Hospital of Lianyungang, Lianyuangang 222000, Jiangsu Province, China. Tel: +86 518 85605152; Fax: +86 518 85605152; E-mail: yangudoc@163.com

References

[1] Jemal A, Siegel R, Ward E, Hao Y, Xu J, Murray T and Thun MJ. Cancer statistics, 2008. CA Cancer J Clin 2008; 58: 71-96.

[2] Kamangar F, Dores GM and Anderson WF. Patterns of cancer incidence, mortality, and prevalence across five continents: defining priorities to reduce cancer disparities in different geographic regions of the world. J Clin Oncol 2006; 24: 2137-2150.

[3] Chung JY, Kitano H, Takikita M, Cho H, Noh KH, Kim TW, Ylaya K, Hanaoka J, Fukuoka J and Hewitt SM. Synaptonemal complex protein 3 as a novel prognostic marker in early stage non-small cell lung cancer. Hum Pathol 2013; 44: 472-479.

[4] Postmus PE. Chemotherapy for non-small cell lung cancer: the experience of the Lung Cancer Cooperative Group of the European Organization for Research and Treatment of Cancer. Chest 1998; 113: 28S-31S.

[5] Travis WD, Brambilla E and Riely GJ. New pathologic classification of lung cancer: relevance for clinical practice and clinical trials. J Clin Oncol 2013; 31: 992-1001.

[6] Cerfolio RJ and Bryant AS. Survival of patients with unsuspected N2 (stage IIIA) nonsmall-cell lung cancer. Ann Thorac Surg 2008; 86: 362-366.

[7] Robinson LA, Ruckdeschel JC, Wagner H Jr and Stevens CW. Treatment of non-small cell lung cancer-stage IIIA: ACCP evidencebased clinical practice guidelines (2nd edition). Chest 2007; 132: 243S-265S.

[8] Zhou H, Xiong Z, Liu J, Chen S, Zhou M and Liu Y. Correlation between podoplanin-positive lymphatic microvessel density and CT characteristics of non-small cell lung cancer. Zhongguo Fei Ai Za Zhi 2012; 15: 34-38.

[9] Yoshizawa A, Motoi N, Riely GJ, Sima CS, Gerald WL, Kris MG, Park BJ, Rusch VW and Travis WD. Impact of proposed IASLC/ATS/ERS classification of lung adenocarcinoma: prognostic subgroups and implica-tions for further revision of staging based on analy-sis of 514 stage I cases. Mod Pathol 2011; 24: 653-664.

[10] Borczuk AC, Qian F, Kazeros A, Eleazar J, Assaad A, Sonett JR, Ginsburg M, Gorenstein L and Powell CA. Invasive size is an independent predictor of survival in pul-monary adenocarcinoma. Am J Surg Pathol 2009; 33: 462-469.

[11] Bhure UN, Lardinois D, Kalff V, Hany TF, Soltermann A, Seifert B and Steinert HC. Accuracy of CT parameters for assessment of tumour size and aggressiveness in lung adenocarcinoma with bronchoalveolar elements. Br J Radiol 2010; 83: 841-849.

[12] Lee HY, Han J, Lee KS, Koo JH, Jeong SY, Kim BT, Cho YS, Shim YM, Kim J, Kim K and Choi YS. Lung adenocar-cinoma as a solitary pulmonary nodule: Prognostic determinants of CT, PET, and histopathologic find-ings. Lung Cancer 2009; 66: 379-385.

[13] Qiao PG, Huang Q, Zhou J, Wang XC, Li M, Ma JL, Tian N and Li GJ. Feasibility of quantitative parameters of dynamically enhanced patterns of spiral computed tomography scanning integrated into tumour progression before targeted treatment of non-small cell lung cancer. J Med Imaging Radiat Oncol 2015; 59: 216-220.

[14] Zhao L, Guan W, Han Y and Zhao Y. Comparative study on CT perfusion parameters of different types of lung cancer before and after chemoradiotherapy. J Biol Regul Homeost Agents 2014; 28: 675-681.

[15] Siva S, Callahan J, Kron T, Martin OA, MacManus MP, Ball DL, Hicks RJ and Hofman MS. A prospective observational study of Gallium-68 ventilation and perfusion PET/CT during and after radiotherapy in patients with non-small cell lung cancer. BMC Cancer 2014; 14: 740.

[16] Folkman J and Shing Y. Angiogenesis. J Bid Chem 1992; 267: 1093l-10934.

[17] Jusufović E, Rijavec M, Keser D, Korošec P, Sodja E, Iljazović E, Radojević Z and Košnik M. let-7b and miR-126 are down-regulated in tumor tissue and correlate with microvessel density and survival outcomes in non--small--cell lung cancer. PLoS One 2012; 7: e45577.

[18] Yu J, Shi R, Zhang D, Wang E and Qiu X. Expression of integrin-linked kinase in lung squamous cell carcinoma and adenocarcinoma: correlation with E-cadherin expression, tumor microvessel density and clinical outcome. Virchows Arch 2011; 458: 99-107.

[19] Tateishi U, Nishihara H, Watanabe S, Morikawa T, Abe K and Miyasaka K. Tumor angiogenesis and dynamic CT in lung carcinoma: radiologic-pathologic correlation. J Comput Assist Tomogr 2001; 25: 23-27.

[20] Trojanowski P, Klatka J, Trojanowska A, Jargiełło T and Drop A. Evaluation of cervical lymph nodes with CT perfusion in patients with hypopharyngeal and laryngeal squamous cell cancer. Pol J Radiol 2011; 76: 7-13.

[21] Lau CL and Harpole DH. Noninvasive clinical staging modalities for lung cancer. Semin Surg Oncol 2000; 18: 116-123.

[22] Medina Gallardo JF, Borderas Naranjo F, Torres Cansino M and Rodriguez-Panadero F. Validity of enlarged mediastinal nodes as markers of involvement by non-small cell lung cancer. Am Rev Respir Dis 1992; 146: 1210-1212.
[23] Kerr KM, Lamb D, Wathen CG, Walker WS and Douglas NJ. Pathological assessment of mediastinal lymph nodes in lung cancer: implications for non-invasive mediastinal staging. Thorax 1992; 47: 337-341.
[24] Vogel P, Daschner H, Lenz J and Schäfer R. Correlation of lymph node size and metastatic involvement of lymph nodes in bronchial cancer. Langenbecks Arch Chir 1990; 375: 141-144.
[25] Pirronti T, Macis G, Sallustio G, Minordi LM, Granone P, Vecchio FM and Marano P. Evaluation of the "N" factor in nonsmall cell lung csncer. Correlation between computerized tomography and pathologic anatomy. Radiol Med 2000; 99: 340-346.
[26] Som PM. Detection of metaslasis in cervical lymphnodes: CT And MR criteria and differential diagnosis. AJR Am J Roentgenol 1992; 158: 961-969.
[27] Macia I, Ramos R, Moya J, Rivas F, Ureña A, Banque M, Escobar I, Rosado G and Rodriguez-Taboada P. Survival of patients with non-small cell lung cancer according to lymph node disease: single pN1 vs multiple pN1 vs single unsuspected pN2. Ann Surg Oncol 2013; 20: 2413-2418.
[28] Wei LX, Zhou RS, Xu HF, Wang JY and Yuan MH. High expression of FOXC1 is associated with poor clinical outcome in non-small cell lung cancer patients. Tumour Biol 2013; 34: 941-946.
[29] Han KY, Gu X, Wang HR, Liu D, Lv FZ and Li JN. Overexpression of MAC30 is associated with poor clinical outcome in human non-small-cell lung cancer. Tumour Biol 2013; 34: 821-825.
[30] Nwogu CE, Yendamuri S, Tan W, Kannisto E, Bogner P, Morrison C, Cheney R, Dexter E, Picone A, Hennon M, Hutson A, Reid M, Adjei A and Demmy TL. Lung cancer lymph node micrometastasis detection using real-time polymerase chain reaction: correlation with vascular endothelial growth factor expression. J Thorac Cardiovasc Surg 2013; 145: 702-707; discussion 707-708.
[31] Memoli JS, El-Bayoumi E, Pastis NJ, Tanner NT, Gomez M, Huggins JT, Onicescu G, Garrett-Mayer E, Armeson K, Taylor KK and Silvestri GA. Using endobronchial ultrasound features to predict lymph node metastasis in patients with lung cancer. Chest 2011; 140: 1550-1556.